

Regiodivergent Hydroborative Ring Opening of Epoxides via Selective C–O Bond Activation

Marc Magre, Eva Paffenholz, Bholanath Maity, Luigi Cavallo,* and Magnus Rueping*



Cite This: *J. Am. Chem. Soc.* 2020, 142, 14286–14294



Read Online

ACCESS |



Metrics & More

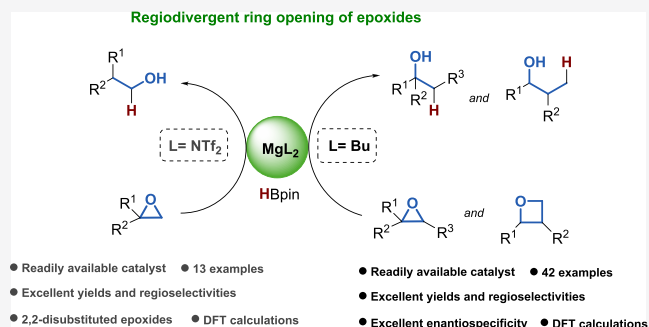


Article Recommendations



Supporting Information

ABSTRACT: A magnesium-catalyzed regiodivergent C–O bond cleavage protocol is presented. Readily available magnesium catalysts achieve the selective hydroboration of a wide range of epoxides and oxetanes yielding secondary and tertiary alcohols in excellent yields and regioselectivities. Experimental mechanistic investigations and DFT calculations provide insight into the unexpected regiodivergence and explain the different mechanisms of the C–O bond activation and product formation.



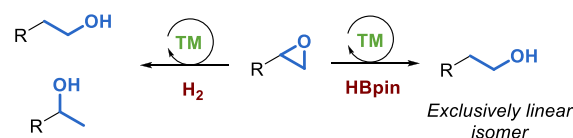
INTRODUCTION

The broad presence of hydroxyl moieties in pharmaceuticals, agrochemicals, and fragrance chemistry have led to the development of efficient protocols for their synthesis.¹ In this regard, epoxides can be easily converted to alcohols via a ring-opening reaction. It is well-known that nonsymmetrical epoxides afford mixtures of regioisomers, where ratios between linear and branched alcohols are strongly dependent on the reducing agent employed.² In past decades, great efforts have been made to overcome regioselectivity problems of the ring-opening reaction of epoxides.² The catalytic C–O bond cleavage is limited because of the high stability of the corresponding metal-alkoxide products, which impedes the regeneration of the metal hydride intermediate.³ One of the most employed catalytic methods for the ring-opening of epoxides is transition-metal-catalyzed hydrogenation, either by using heterogeneous or homogeneous catalysts.⁴ In all cases, high temperatures and H₂ pressures are required, leading to poor selectivity along with the generation of oligomers or saturated hydrocarbons as byproducts (Scheme 1a). In recent years, the transition-metal-catalyzed hydroboration has appeared as a plausible alternative to the hydrogenation protocols. The use of the mild reductant pinacolborane resulted in good selectivities, however, exclusively toward linear alcohols (Scheme 1a).⁵

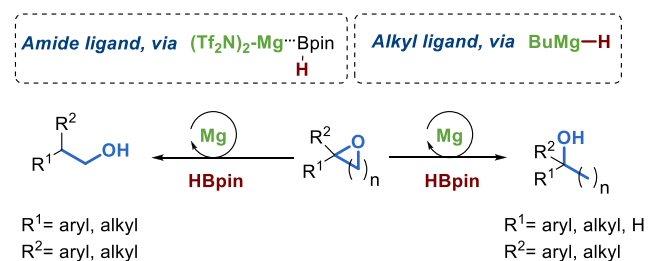
Alkaline-earth metals are among the most abundant metals in the crust of the earth. Despite their abundance and low toxicity, their application has been mainly focused on the hydrofunctionalization of polarized unsaturated bonds.^{6,7} Since the first structurally characterized magnesium–hydride complex by Jones and Stasch and co-workers,⁸ great efforts have been carried out to understand the Mg–H reactivity and its application as a valuable alternative to transition-metal hydride

Scheme 1. Catalytic Methods for the Regioselective Ring Opening of Epoxides

a) Catalytic hydrogenation and hydroboration of epoxides



b) This work: Ligand-controlled regiodivergent hydroboration



species.⁶ As a result, magnesium complexes, mostly containing anionic β -diketiminato ligands,⁹ have been successfully applied to the hydroboration of polarized and unpolarized unsaturated

Received: May 31, 2020

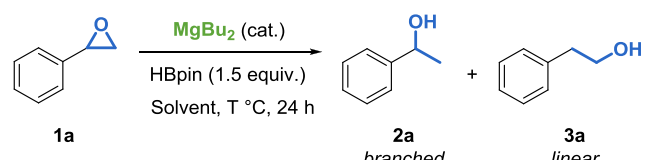
Published: July 13, 2020



bonds.¹⁰ In certain cases, even low-cost and readily available dialkylmagnesium could be applied as a catalyst.¹¹ Given the current limitations in the catalytic regiodivergent ring opening of epoxides, we decided to explore whether simple magnesium catalysts would allow for the selective C–O bond activation, leading to either branched or linear alcohols in good yields and with broad functional group tolerance (Scheme 1b). We here report the development of such a regiodivergent reaction and explain the mechanism supported by experiment and computation.

We began our investigations with the magnesium-catalyzed hydroboration of styrene oxide **1a** by evaluating the activity and selectivity of readily available MgBu_2 (Table 1). When the

Table 1. Reaction Optimization^a



entry	MgBu_2 (mol %)	T (°C)	solvent	2a:3a (b:l) ^c	conv. (%) ^d
1	10	50	toluene	80:20	99
2	5	50	toluene	80:20	99
3	5	40	toluene	84:16	99
4	5	40	THF	87:13	99
5 ^b	5	40	THF	89:11	99 (95)
6	5	40	neat	66:33	99
7		40	THF	n.d.	<5

^a**1a** (1 mmol), HBpin (1.5 equiv.), MgBu_2 (0.5 M in heptane), solvent [1 M] for 24 h. ^bTHF [0.5 M]. ^cSelectivities determined by ¹H NMR. ^dConversions determined by GC. Isolated yield in parentheses.

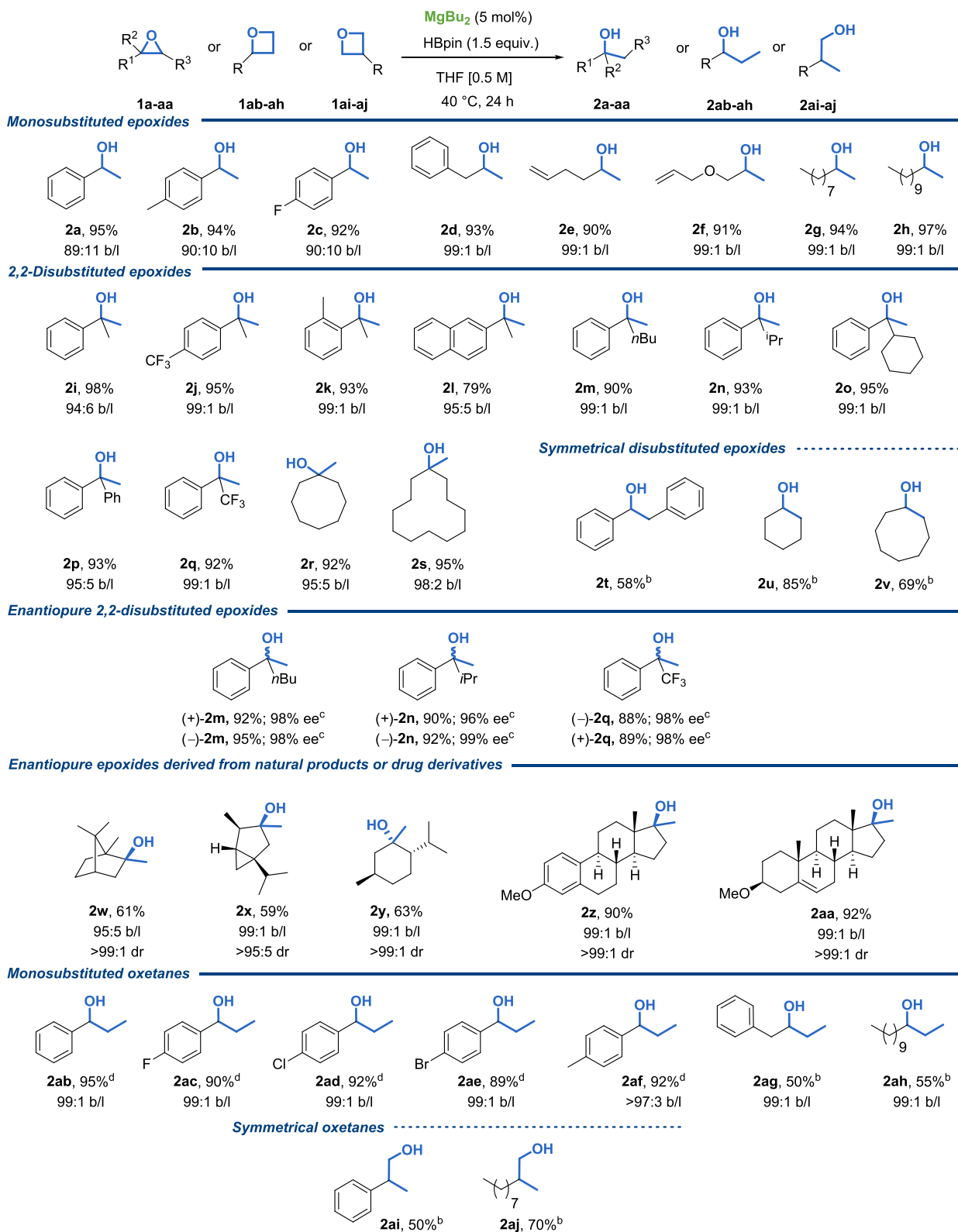
catalyst loading was decreased, the activity was maintained (Table 1 entry 1 vs 2). Whereas all catalytic methods for the hydroboration of epoxides provided the linear regioisomer,⁵ the magnesium catalyst provided the branched product. The regioselectivity could be improved by decreasing the reaction temperature (Table 1, entry 2 vs entry 3). Testing different solvents led to a small increase in regioselectivity when THF was used (Table 1, entry 4). Finally, by decreasing the reaction concentration (Table 1, entry 5), we reached better results. It should be pointed out that performing the catalytic reaction in neat conditions (Table 1, entry 6) resulted in a lower regioselectivity.

Following this optimization, we explored the scope and limitations of the MgBu_2 -catalyzed regioselective hydroboration of epoxides (Scheme 2) starting with monosubstituted terminal epoxides, which lead to secondary alcohols (**2a–2h**). When aromatic substituents are present, good to excellent regioselectivities were obtained, regardless of the electronic nature of the aromatic moiety. Use of epoxides bearing an alkyl substituent (**1d–1h**) showed full regioselectivity and good yields. On the basis of the good performance observed, also substrates with alkenyl moieties (**1e–1f**) were tested. Fortunately, no influence on the chemoselectivity toward the C–O cleavage was observed and the products were isolated in good yields. Encouraged by these results, we decided to test disubstituted terminal epoxides (**1i–1s**). In this case, tertiary alcohols, important synthesis building blocks also found in several natural products,¹² were obtained in excellent yields and regioselectivities. Again, different electronic and steric

properties on the aryl group (**2i–2l**) did not influence either the activities or selectivities. When different alkyl-substituted substrates (**2m–2o**) were applied, excellent results were preserved. Interestingly, diphenyl epoxide **1p** also underwent hydroboration regioselectively. In a similar manner, the MgBu_2 -catalyzed hydroboration of trifluoromethyl-containing epoxide **1q** also provided exclusively the branched alcohol **2q** in excellent yields and regioselectivities. We were delighted to see that this good performance could also be extended to epoxides present in macrocycles, affording in all cases the tertiary alcohols **2r** and **2s** in excellent yields and regioselectivities. When symmetrical disubstituted epoxides were studied (**1t–1v**), the corresponding alcohols **2t–2v** could be isolated in good yields, although higher temperatures were required.

Tertiary alcohols are present in several natural products or drug derivatives.¹² Thus, the synthesis of enantiomerically pure tertiary alcohols is of great interest. In this regard a few catalytic asymmetric reactions are known,¹³ with the catalytic asymmetric addition of carbon-nucleophiles to ketones as the most synthetically used approach.¹⁴ Motivated by the above results, we decided to test the MgBu_2 -catalyzed hydroboration protocol for both (*R*)- and (*S*)-enantiomers of 2,2-disubstituted epoxides **1m–1n** and **1q**. Importantly, no loss of enantiomeric excess was observed and the tertiary alcohols were in optically pure form. This good performance was also extended when chiral epoxides derived from natural products or drug derivatives were tested under the same reaction conditions. When *L*-camphor (**1w**)-, α -thujone (**1x**)-, and *L*-menthone (**1y**)-derived epoxides were studied, good yields and excellent regio- and diastereoselectivities were obtained. We were also pleased to see that sterol-derived epoxides **1z** and **1aa** also underwent hydroboration effectively with excellent yields and regio- and diastereoselectivities.

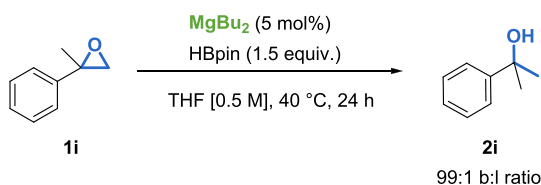
The findings make us wonder whether less reactive oxacyclic rings, such as oxetanes and oxolanes, could also be applied in the Mg-catalyzed ring opening. To the best of our knowledge, there is no catalytic method reported for the hydroboration reaction involving these unreactive compounds. To our delight, the hydroboration could also be applied and monosubstituted oxetanes containing aryl substituents (**1ab–1af**) underwent ring opening to give the corresponding branched alcohols **2ab–2af** in good yields and excellent regioselectivities. This good performance was also maintained when alkyl substituents are present at the 2-position (**1ag–1ah**), although lower conversions were observed. When symmetrical oxetanes **1ai–1aj** were tested, the corresponding alcohols **2ai–2aj** were also isolated in moderate to good yields. Encouraged by these results, we decided to study the MgBu_2 -catalyzed hydroboration of 2-phenyloxolane. Unfortunately, even under harsher reaction conditions, no conversion was observed for these less reactive oxacycles. Thus, we wondered if the replacement of the ligand (i.e., butyl) would have an effect on the catalytic activity. Inspired by our recent findings in which (i) $\text{Mg}(\text{OR})_2$ (where $(\text{OR})_2 = \text{BINOL}$) was shown to activate HBpin toward ketone reduction via a cooperative magnesium-ligand activation,^{15a} and (ii) $\text{Mg}(\text{NTf}_2)_2$ acting as an efficient Lewis acid toward alkyne activation,^{15b} we decided to replace MgBu_2 by $\text{Mg}(\text{NTf}_2)_2$ and to evaluate the influence on both the activity and the selectivity. To our surprise, the application of $\text{Mg}(\text{NTf}_2)_2$ in the hydroboration of 2,2-disubstituted epoxide **1i** resulted in the linear alcohol product **4a** (**2ai**) (Scheme 3).

Scheme 2. Scope of the MgBu_2 -Catalyzed Hydroboration of Epoxides and Oxetanes^a

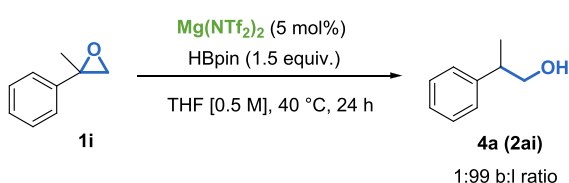
^a**1a–1aj** (1 mmol), HBpin (1.5 equiv), MgBu_2 (5 mol %, 0.5 M in heptane), THF [0.5 M], 40 °C for 24 h. Isolated yields. ^bToluene [1 M], 10 mol % MgBu_2 , 90 °C. ^cEnantioselectivities were determined by HPLC. Diastereoselectivities were determined by ¹H NMR. (*R*)- and (*S*)-**1m**, (*S*)-**1n**, and (*R*)- and (*S*)-**1o** epoxides were used in 99% ee purity. (*R*)-**1n** epoxide was used in 97% ee purity (all isolated from preparative HPLC; for more information, see Supporting Information). Epoxides **1w**, **1x**, **1y**, **1z**, and **1aa** were diastereomerically pure. ^d MgBu_2 (5 mol %, 0.5 M in heptane), toluene [1 M], 75 °C for 24 h.

Scheme 3. Regiodivergent Magnesium-Catalyzed Hydroboration of Epoxides

a) $MgBu_2$ -catalyzed hydroboration of epoxides: **Branched isomer**



b) $Mg(NTf_2)_2$ -catalyzed hydroboration of epoxides: **Linear isomer**



This complete regioselectivity switch is very interesting and points to a different HBpin activation and ring-opening mechanism. Several 2,2-disubstituted terminal epoxides with sterically hindered or polyaromatic ring substitutions (**4b** and **4c**) as well as linear and cyclic alkyl substituents (**4d–4l**) were then applied (Scheme 4). The scope could also be extended diaryl-substituted substrate and 2,2-diphenylethan-1-ol **4m** was obtained quantitatively. Overall, the $Mg(NTf_2)_2$ -catalyzed hydroboration results in good yields and complete selectivity toward linear alcohols.

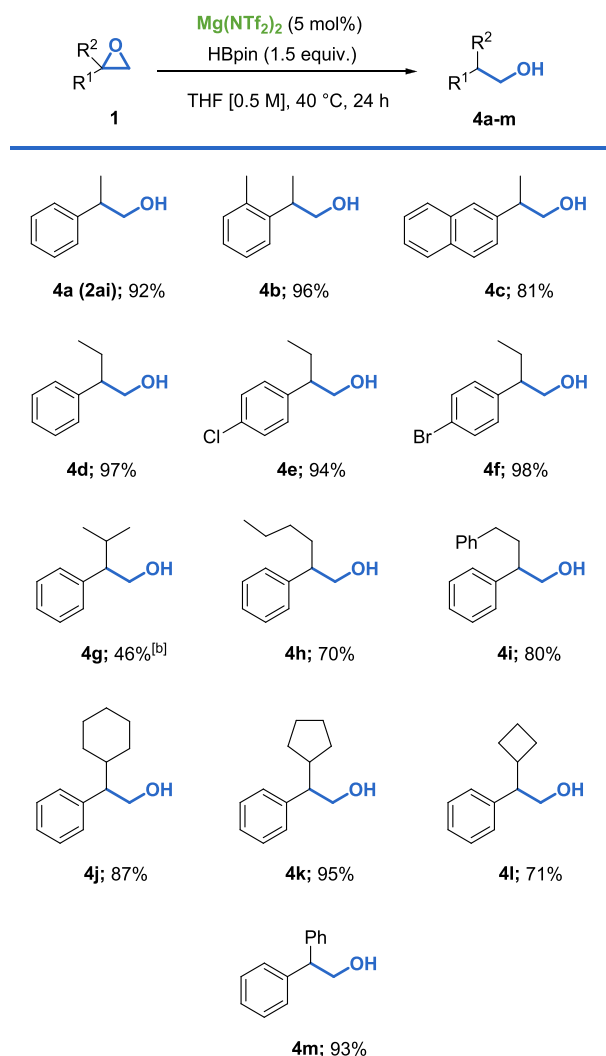
Thus, we successfully developed a regiodivergent ring opening of epoxides by applying two readily available and low-cost magnesium catalysts. On one hand, our $MgBu_2$ –HBpin catalytic system can be applied to a broad range of substrates providing branched alcohols with excellent chemo- and regioselectivities without the loss of enantioselectivity. On the other hand, the use of $Mg(NTf_2)_2$ as catalyst provides the complementary ring-opening reaction leading to the linear alcohols. Considering the unexpected regiodivergence observed by using either $MgBu_2$ or $Mg(NTf_2)_2$, we decided to conduct several experiments to gain insight into the different reaction mechanisms (Scheme 5).

MECHANISTIC STUDY

Control Experiments. We assumed that the regiodivergency is caused by the nature of the different magnesium catalysts. However, given that BH_3 is capable of catalyzing the hydroboration of olefins,¹⁶ and due to examples in the literature that describe the decomposition of HBpin to BH_3 by alkali salts,¹⁷ we decided to investigate if BH_3 could catalyze the hydroboration of epoxides to either a linear or branched alcohol. Therefore, BH_3 ·THF and BH_3 ·SMe₂ were tested in the reaction. However, both did not efficiently catalyze the hydroboration (Scheme 5a), providing low conversions and a mixture of branched and isomerization byproduct (for more detail, see the Supporting Information). Subsequently, we investigated the deuterium incorporation by using DBpin (Scheme 5b).

When the $MgBu_2$ -catalytic system was tested, the secondary alcohol **2d-d₁** was isolated with full D-incorporation at the β-methyl moiety. This result suggested that the $BuMg$ -D species in situ formed would attack the least substituted carbon of the epoxide ring (Scheme 5b1). Moreover, no isomerization was observed. We also carried out the same D-incorporation

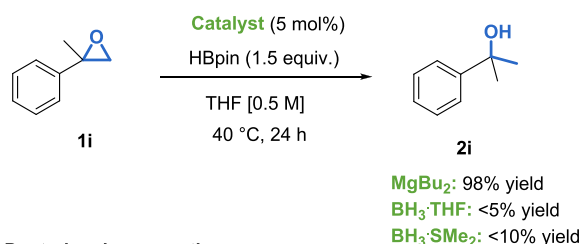
Scheme 4. $Mg(NTf_2)_2$ -Catalyzed Hydroboration of Epoxides^a



^a **1** (1 mmol), $Mg(NTf_2)_2$ (5 mol%), HBpin (1.5 equiv) in THF [0.5 M] at 40 °C for 24 h. ^b $Mg(NTf_2)_2$ (10 mol %).

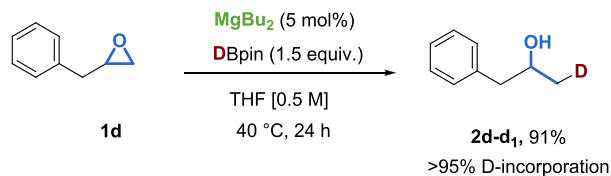
experiments by using $Mg(NTf_2)_2$. In this case, quantitative D-incorporation was observed at the less substituted carbon (Scheme 5b2). This result, together with the complete regiodivergence observed, suggests that the latter mechanism operates via a 1,2-H shift,^{18a} producing an aldehyde intermediate, which finally undergoes reduction via a D-addition. This epoxide isomerization is in agreement with the work reported by Weinwald^{18a} and Mazet using Pd or Ir catalysts.^{18b,c} Consequently, we carried out an isomerization experiment (Scheme 5c). When epoxide **1i** was mixed with catalytic amounts of $Mg(NTf_2)_2$ complex, we observed the formation of aldehyde **5**. This result supports the notion that Lewis acidic $Mg(NTf_2)_2$ is an efficient catalyst for the Meinwald rearrangement (1,2-H shift)^{18a} of terminal disubstituted epoxides to the corresponding aldehyde, which is in agreement with the control experiments (Scheme 5b2). Finally, we conducted a racemization experiment (Scheme 5d). As shown, $MgBu_2$ catalyzes the ring opening of an enantiopure epoxide without loss of enantioselectivity (Scheme 2, compounds **2m**, **2n**, and **2q**). When enantiopure epoxide **1m** was tested in the presence of $Mg(NTf_2)_2$ catalyst,

Scheme 5. Control Experiments

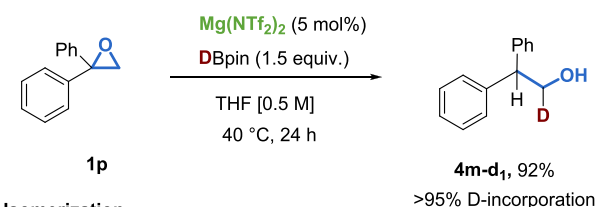
a) BH_3 as catalyst for the hydroboration of epoxides

b) Deuterium incorporation

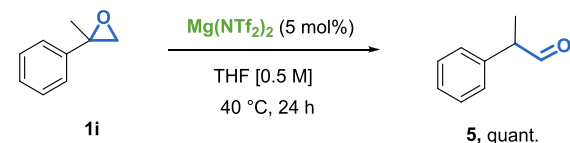
b1)



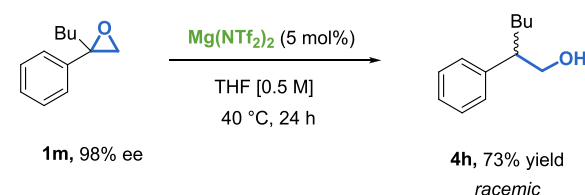
b2)



c) Isomerization



d) Racemization



rac-**4h** was obtained, which can be explained by the formation of a carbocation intermediate.

Computational Study. Supported by control experimental results, we performed DFT calculations (Computational Details in the Supporting Information) to define possible reaction pathways for both catalytic systems, MgBu_2 and $\text{Mg}(\text{NTf}_2)_2$. Epoxide **1i** was selected as the prototype substrate.

MgBu_2 -Catalyzed Mechanism. As previously reported, hydroboration reactions using MgBu_2 as the catalyst occur via in situ formation of the active catalytic species BuMg-H .¹¹ The energy profile for the formation of BuMg-H by the reaction of MgBu_2 with HBpin is discussed in Figure S1 (see the Supporting Information). Within the reaction conditions used in this work, BuMg-H can be stabilized by solvent molecules (THF), by HBpin, or by **1i**, as shown in Figure S2. Among all the possibilities, the most stable geometry is A_7 , in which two THF molecules are coordinated to Mg, and we

considered it as the starting state in the catalytic cycle. The overall pathway is divided into two sections: ring opening of the epoxide (Figure 1) and metathesis of the Mg–O and H–B bonds (Figure 2).

Calculations indicate that a bimolecular ring-opening mechanism is operative; see Figure 1. The reaction pathway starts with the transfer of a hydride from A_7 to an epoxide molecule coordinated to the Mg of another A_7^h molecule, via the transition state of **TS1**. This bimolecular epoxide ring-opening step is required to overcome a free energy span of 24.0 kcal/mol from the reference state corresponding to two A_7 molecules. The resulting ionic intermediates A_8 and A_9 are 27.5 kcal/mol lower in energy than the starting two A_7 molecules. The next two steps, from $\text{A}_8 + \text{A}_9$ to $\text{A}_{10} + \text{A}_{11}$, correspond to substantially thermoneutral dissociation of a THF molecule from A_9 , yielding A_{10} , and to substitution of a THF molecule of A_8 by an epoxide molecule, yielding A_{11} . The reaction proceeds by another epoxide opening by hydride transfer from A_{10} to A_{11} via another bimetallic transition state, **TS2**. This ring opening is clearly more facile ($\Delta G^\ddagger = 9.0$ kcal/mol) than that via **TS1** ($\Delta G^\ddagger = 24.0$ kcal/mol). The reason for this observation is the attractive electrostatic interaction between the two oppositely charged A_{10} and A_{11} . The resulting two molecules of A_{12} are highly stable, laying at -108.3 kcal/mol with respect to starting A_7 . Intermediate A_{12} , having two THF molecules coordinated to the Mg, is the most stable over other possibilities (see Figure S3 in the Supporting Information). The next step, metathesis of the Mg–O and B–H bonds, starts with the replacement of one THF of intermediate A_{12} by HBpin to generate A_{12}^h , a step endergonic by 3.4 kcal/mol (Figure 2). Then the alkoxide group migrates to the boron atom via transition state **TS3** and a total energy barrier of 5.6 kcal/mol from A_{12} . The resulting zwitterionic intermediate A_{13} is highly stable and is the lowest point in the potential energy surface. The reaction is completed by hydride transfer from the electron-rich HBpin moiety to the electron-deficient Mg center of A_{13} , via transition state **TS4** and an energy barrier of 19.9 kcal/mol. Liberation of product P_A from the formed intermediate A_{14} regenerates A_7 for further catalysis. The overall reaction profile (Figures 1 and 2) reveals that bimetallic hydride transfer via **TS1** is the rate-controlling step. Regarding the regioselectivity, we checked the two epoxide opening transition states **TS1** and **TS2**. We thus investigated the hydride transfer step via **TS1-R** and via **TS2-R**, where hydride transfer occurs to the substituted C atom of the epoxide (red lines in Figure 1). Consistent with the experimental regioselectivity, transition states **TS1** and **TS2** are favored by 5.2 and 3.8 kcal/mol as compared to transition states **TS1-R** and **TS2-R** (details in Figure S4 in the Supporting Information). The high regioselectivity toward H transfer to the unsubstituted C atom of the epoxide can be easily rationalized in terms of steric effects. In fact, the steric map of the epoxide coordinated intermediate A_7^h (Figure 3) shows that, as expected, the western quadrants, hosting the unsubstituted C atom of the epoxide, are less hindered than the eastern ones, hosting the substituted C atom.¹⁹

The catalytic pathway examined by the DFT calculations reveals an explicit role for the THF solvent molecules coordinated to Mg. Therefore, we investigated the feasibility of this mechanism with a noncoordinating solvent, for example, toluene. In this case the starting Mg–H complex is A_7^e , in which two molecules of HBpin are bound to the Mg (Figure S5 in the Supporting Information). The resulting

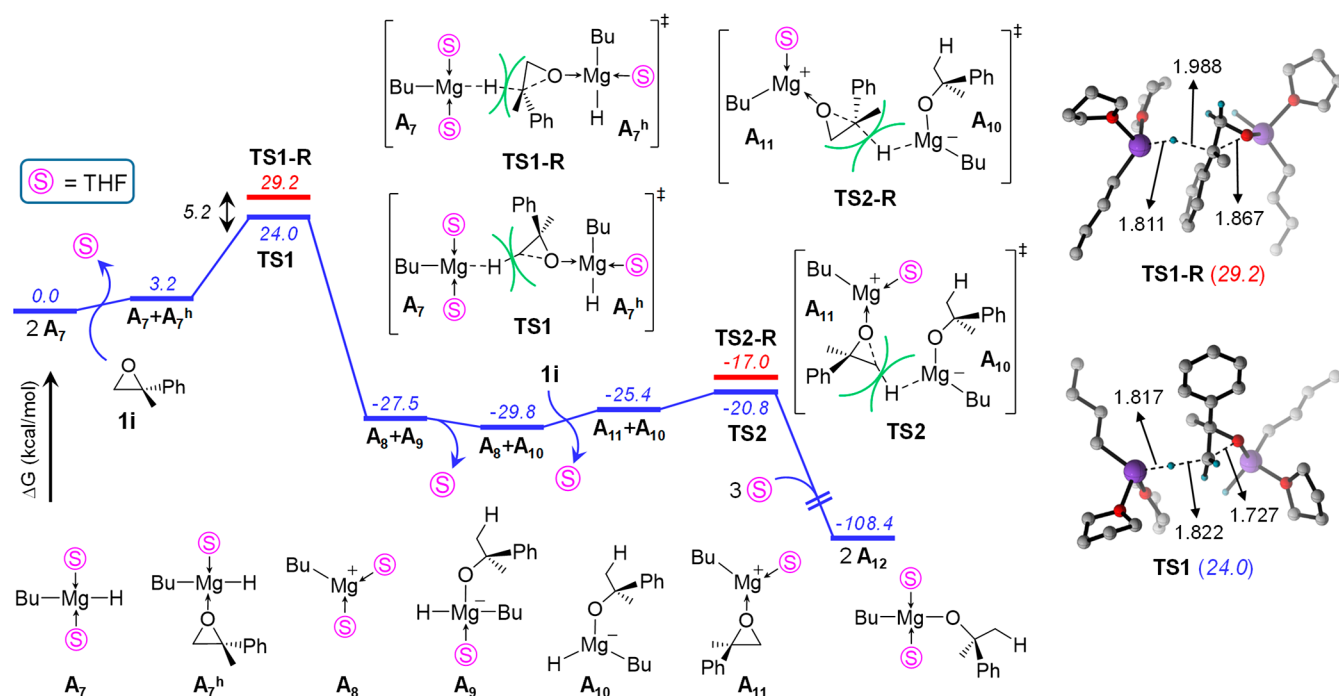


Figure 1. Computed energy profile for the ring-opening step in MgBu_2 -catalyzed hydroboration of the epoxide reaction. Free energy values at M06-2X(SMD, THF solvent)/Def2-TZVP//PBE0/Def2-SVP level of theory are presented.

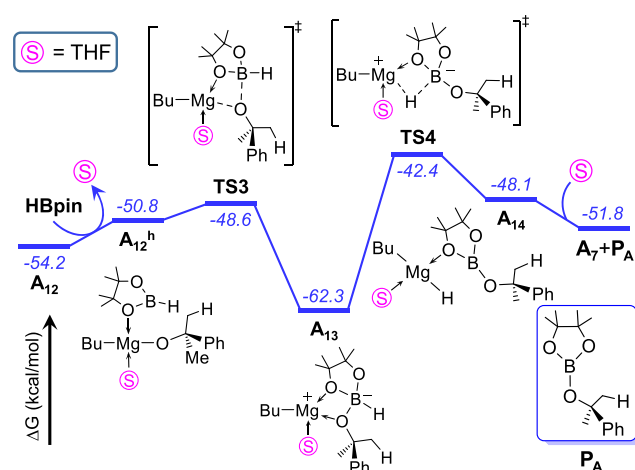


Figure 2. Computed energy profile for the metathesis of Mg-O and B-H bonds in MgBu_2 -catalyzed hydroboration of the epoxide reaction. For energy convention refer to [Figure 1](#).

activation energy barrier for the hydride transfer step via **TS1**, 22.5 kcal/mol, is similar to that reported in [Figure 1](#). Furthermore, hydride transfer to the substituted C atom of the epoxide, via transition state **TS1-R**, is unfavored by 2.3 kcal/mol relative to **TS1**. Thus, the proposed mechanism can be considered operative both in coordinating and non-coordinating solvents.

$\text{Mg}(\text{NTf}_2)_2$ -Catalyzed Mechanism. Also in this case we started by analyzing the most stable form of the $\text{Mg}(\text{NTf}_2)_2$ catalyst in the presence of substrate **1i** and HBpin (for details, refer to [Figure S6](#) in the Supporting Information). The complex **B₁**, having two THF molecules coordinated to the Mg atom, is found to be the most stable form and it is considered as the starting point of the reaction pathway. Different from the MgBu_2 -catalyzed mechanism, the formation of the Mg-H

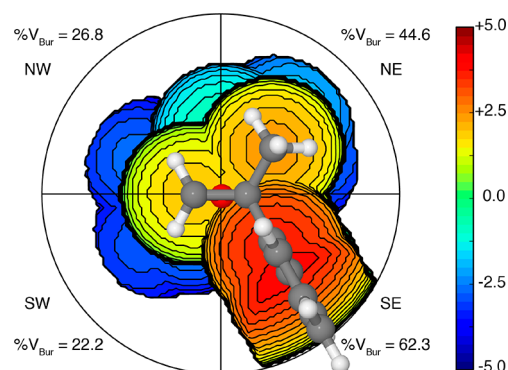


Figure 3. Steric map of the epoxide-coordinated intermediate **A₇^h**. The percentage of buried volume is reported near each of the quadrants. For clarity, the 3D geometry of the coordinated epoxide is overlapped on the steric map. The scale of the steric contours is also reported. The middle point of the epoxide C-C bond is placed at the origin, and the epoxide O atom is placed on the Z-axis.

complex is unfeasible because of the very high endergonicity associated with the transfer of a hydride from HBpin to Mg ($\Delta G^\ddagger = 37.8$ kcal/mol, [Scheme S1](#) in the Supporting Information). Thus, for $\text{Mg}(\text{NTf}_2)_2$ -catalyzed hydroboration we had to locate an alternative mechanism, devoid of a Mg-H intermediate. The overall reaction pathway is composed of two steps: isomerization of epoxide to aldehyde, followed by hydroboration of the aldehyde ([Figure 4](#)).

The reaction starts with the replacement of a THF in **B₁** by the epoxide molecule **1i** generating **B₁^b**, a step endergonic by 5.5 kcal/mol. The next step is ring opening of the epoxide by nucleophilic attack via the $\text{S}_{\text{N}}2$ -type transition state **TS5** ([Figure 4](#)). This step requires the overcoming of a free energy barrier of 29.2 kcal/mol from **B₁** and leads to the formation of the intermediate **B₂**, a charge-separated species. The high-energy intermediate **B₂** transforms rapidly to the aldehyde-

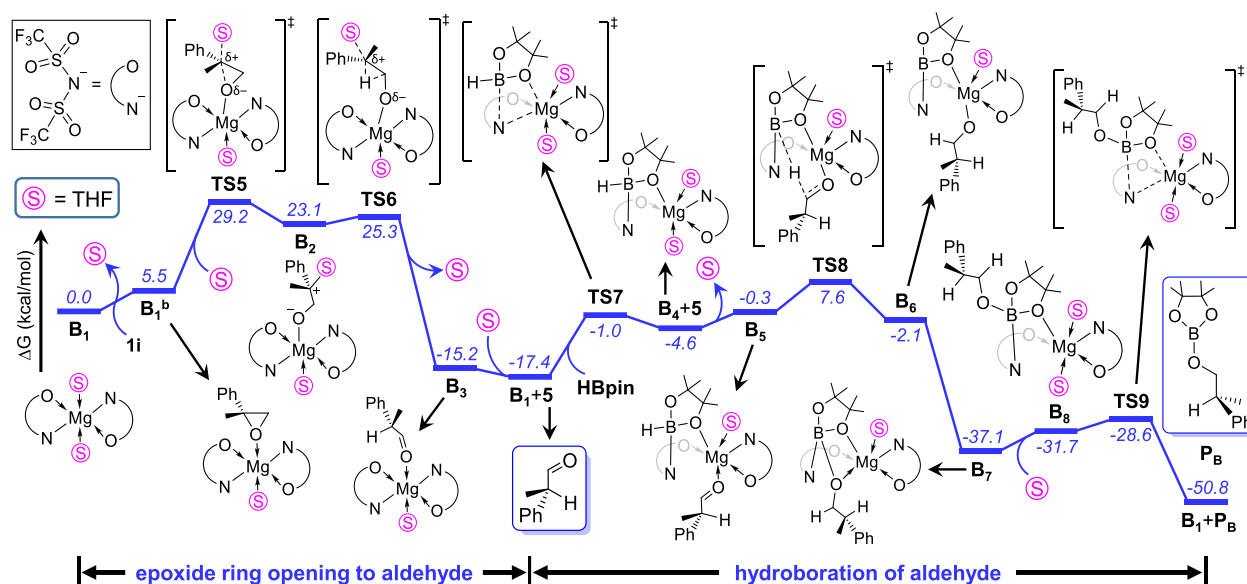


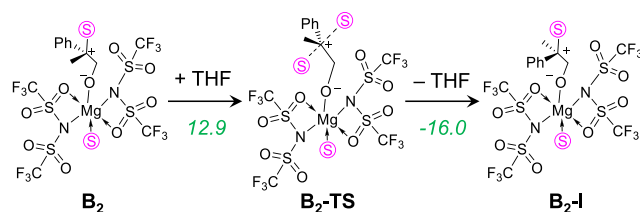
Figure 4. Computed energy profile for the $\text{Mg}(\text{NTf}_2)_2$ -catalyzed ring-opening hydroboration of epoxide. For energy convention refer to Figure 1.

coordinated species B_3 via the 1,2-H transfer transition state TS_6 , with a negligible activation barrier ($\Delta G^\ddagger = 2.2$ kcal/mol). Coordination of a THF molecule to B_3 liberates the aldehyde **5** and regenerates B_1 .

Hydroboration of the aldehyde starts with HBpin insertion into one of the $\text{Mg}-\text{N}(\text{NTf}_2)$ bonds of B_1 , via TS_7 and a free energy barrier of 16.4 kcal/mol, to form intermediate B_4 . One THF molecule of B_4 is replaced by **5** to generate B_5 , which is less stable than B_4 by 4.3 kcal/mol. Hydride transfer from the electron rich HBpin in B_4 to the coordinated $\text{C}=\text{O}$ of **5**, occurs via transition state TS_8 and leads to intermediate B_6 . This step requires the overcoming of an overall free energy span of 25.0 kcal/mol from the reference structures $\text{B}_1+\mathbf{5}$. The next step is a barrier less and highly exergonic ($\Delta G = -35.0$ kcal/mol) rearrangement of B_6 to B_7 , corresponding to nucleophilic transfer of the alkoxide group from magnesium to boron. The reaction is completed by release of product P_B , promoted by coordination of a THF molecule to Mg, via transition state TS_9 and an energy barrier of 8.5 kcal/mol, regenerating the active catalyst B_1 .

To rationalize the experimentally observed loss of enantioselectivity in the product, when the reaction is catalyzed by $\text{Mg}(\text{NTf}_2)_2$, we investigated racemization (see Scheme 6). The reaction starts with the Mg-coordinated alkoxide B_2 , which is predicted to be the structure from which racemization starts. In B_2 , the THF is coordinated to the cationic carbon, which is a chiral center. This THF can be replaced with another THF via $\text{S}_\text{N}2$ -type transition state. Therefore, an

Scheme 6. Energetics for the Step of Racemization of $\text{Mg}(\text{NTf}_2)_2$ -Catalyzed Reaction



inversion of configuration is observed at the chiral center in the resulting intermediate, emerging a pathway toward the formation of enantiomer of P_B .

CONCLUSIONS

In summary, a new magnesium-catalyzed protocol has been successfully applied to a wide range of terminal and internal epoxides. Depending on the nature of the Mg catalyst, a regiodivergent ring opening is observed. Whereas MgBu_2 provides the corresponding branched alcohol, $\text{Mg}(\text{NTf}_2)_2$ allows the formation of the linear regioisomer. To date, all transition-metal-catalyzed hydroborations of epoxides protocols provide the linear alcohol. In contrast, the use of readily available MgBu_2 catalyzes the hydroboration of terminal and internal epoxides in excellent regioselectivities toward the branched isomer. Moreover, enantiopure alcohols can also be obtained as a result of the enantiospecific ring opening of optically pure epoxides. Besides, good efficiency is also observed when less reactive oxetanes are applied, which again result in the branched alcohols in good yields and with excellent regioselectivities. To the best of our knowledge, this is the first selective hydroboration of these unreactive compounds. Also, the use of readily available $\text{Mg}(\text{NTf}_2)_2$, containing trifluoromethanesulfonimide ligands, provides the linear isomer when 2,2-disubstituted terminal epoxides were tested.

By means of control experiments and DFT calculations, we demonstrate that the different activation modes of HBpin are crucial for the regiodivergency observed. Mechanistically, for the MgBu_2 -catalyzed procedure a bimolecular ring-opening mechanism is proposed in which the epoxide activation and the hydride addition to the least substituted carbon occur simultaneously, providing the corresponding branched alcohols. Also, the Lewis acid $\text{Mg}(\text{NTf}_2)_2$ facilitates the ring opening of epoxides via an isomerization pathway to give the corresponding aldehyde, which subsequently undergoes hydroboration through a dual magnesium-ligand cooperative HBpin activation. Because of the mild reaction conditions, the use of readily available and nontoxic catalysts, the good chemo-, regio-, and stereoselectivities obtained for a wide range of

epoxides, the catalytic system presented can be considered a green alternative to the existing ring-opening protocols and may be further applied to late-stage functionalizations.

■ ASSOCIATED CONTENT

SI Supporting Information

The Supporting Information is available free of charge at <https://pubs.acs.org/doi/10.1021/jacs.0c05917>.

Experimental procedures and analytical data for all compounds, detailed control experiments and DFT calculations, and NMR spectra (PDF)

■ AUTHOR INFORMATION

Corresponding Authors

Luigi Cavallo – KAUST Catalysis Center (KCC), King Abdullah University of Science and Technology (KAUST), Thuwal 23955-6900, Saudi Arabia; orcid.org/0000-0002-1398-338X; Email: luigi.cavallo@kaust.edu.sa

Magnus Rueping – KAUST Catalysis Center (KCC), King Abdullah University of Science and Technology (KAUST), Thuwal 23955-6900, Saudi Arabia; orcid.org/0000-0003-4580-5227; Email: magnus.rueping@kaust.edu.sa

Authors

Marc Magre – Institute of Organic Chemistry, RWTH Aachen, Aachen 52074, Germany; orcid.org/0000-0002-5950-4129

Eva Paffenholz – Institute of Organic Chemistry, RWTH Aachen, Aachen 52074, Germany

Bholanath Maity – KAUST Catalysis Center (KCC), King Abdullah University of Science and Technology (KAUST), Thuwal 23955-6900, Saudi Arabia; orcid.org/0000-0001-5969-0112

Complete contact information is available at: <https://pubs.acs.org/doi/10.1021/jacs.0c05917>

Notes

The authors declare no competing financial interest.

■ ACKNOWLEDGMENTS

We thank Frau Cornelia Vermeeren for preparative HPLC separation. The Deutsche Bundesstiftung Umwelt (DBU) is acknowledged for financial support for E. Paffenholz. We acknowledge the King Abdullah University of Science and Technology (KAUST) for support and the KAUST Supercomputing Laboratory for providing computational resources of the supercomputer Shaheen II.

■ REFERENCES

- (1) Weissmehl, K.; Arpe, H.-J. *Industrial Organic Chemistry*, 4th ed.; Wiley-VCH: Hoboken, NJ, 2008.
- (2) (a) House, H. O. *Modern Synthetic Reactions*; W.A. Benjamin: Menlo Park, CA, 1972; Chapters 1–4. (b) Huang, C.-Y.; Doyle, A. G. The Chemistry of Transition Metals with Three-Membered Ring Heterocycles. *Chem. Rev.* **2014**, *114*, 8153–8198.
- (3) Chong, C. C.; Kinjo, R. Catalytic Hydroboration of Carbonyl Derivatives, Imines, and Carbon Dioxide. *ACS Catal.* **2015**, *5*, 3238–3259.
- (4) For selected examples on hydrogenation of epoxides, see: (a) Newman, M. S.; Underwood, G.; Renoll, M. The Reduction of Terminal Epoxides. *J. Am. Chem. Soc.* **1949**, *71*, 3362–3363. (b) Ley, S. V.; Mitchell, C.; Pears, D.; Ramarao, C.; Yu, J.-Q.; Zhou, W. Recyclable Polyurea-Microencapsulated Pd(0) Nanoparticles: an

Efficient Catalyst for Hydrogenolysis of Epoxides. *Org. Lett.* **2003**, *5*, 4665–4668. (c) Kwon, M. S.; Park, I. S.; Jang, J. S.; Lee, J. S.; Park, J. Magnetically Separable Pd Catalyst for Highly Selective Epoxide Hydrogenolysis under Mild Conditions. *Org. Lett.* **2007**, *9*, 3417–3419. (d) O, W. W. N.; Lough, A. J.; Morris, R. H. The Hydrogenation of Molecules with Polar Bonds Catalyzed by a Ruthenium(II) Complex Bearing a Chelating N-Heterocyclic Carbene with a Primary Amine Donor. *Chem. Commun.* **2009**, *46*, 8240–8242. (e) Liu, W.; Li, W.; Spannenberg, A.; Junge, K.; Beller, M. Iron-catalysed Regioselective Hydrogenation of Terminal Epoxides to Alcohols under Mild Conditions. *Nat. Catal.* **2019**, *2*, 523–528. (f) Yao, C.; Dahmen, T.; Gansäuer, A.; Norton, J. Anti-Markovnikov Alcohols via Epoxide Hydrogenation through Cooperative Catalysis. *Science* **2019**, *364*, 764–767.

(5) For examples on catalytic hydroboration of epoxides, see: (a) Yakabe, S. One-Pot System for Reduction of Epoxides using NaBH₄, PdCl₂ Catalyst and Moist Alumina. *Synth. Commun.* **2010**, *40*, 1339–1344. (b) Desnoyer, A. N.; Geng, J.; Drover, M. W.; Patrick, B. O.; Love, J. A. Catalytic Functionalization of Styrenyl Epoxides via 2-Nickela(II)oxetanes. *Chem. - Eur. J.* **2017**, *23*, 11509–11512. (c) Song, H.; Ye, K.; Geng, P.; Han, X.; Liao, R.; Tung, C.-H.; Wang, W. Activation of Epoxides by a Cooperative Iron–Thiolate Catalyst: Intermediacy of Ferrous Alkoxides in Catalytic Hydroboration. *ACS Catal.* **2017**, *7*, 7709–7717. (d) Patnaik, S.; Sadow, A. D. Interconverting Lanthanum Hydride and Borohydride Catalysts for C = O and C–O Bond Cleavage. *Angew. Chem., Int. Ed.* **2019**, *58*, 2505–2509.

(6) For recent reviews on the use of organomagnesium catalysts, see: (a) Crimmin, M. R.; Hill, M. S. Homogeneous catalysis with organometallic complexes of group 2. *Top. Organomet. Chem.* **2013**, *45*, 191–241. (b) Revunova, K.; Nikonov, G. I. Main Group Catalysed Reduction of Unsaturated Bonds. *Dalton Trans.* **2015**, *44*, 840–866. (c) Rochat, R.; Lopez, M. J.; Tsurugi, H.; Mashima, K. Recent Developments in Homogeneous Organomagnesium Catalysis. *ChemCatChem* **2016**, *8*, 10–20. (d) Hill, M. S.; Liptrot, D. J.; Weetman, C. Alkaline Earths as Main Group Reagents in Molecular Catalysis. *Chem. Soc. Rev.* **2016**, *45*, 972–988.

(7) For illustrative examples using magnesium organometallics for deprotonation/metalation reactions, see: (a) Dong, Z.; Clososki, G. C.; Wunderlich, S. H.; Unsinn, A.; Li, J.; Knochel, P. Direct Zincation of Functionalized Aromatics and Heterocycles by Using a Magnesium Base in the Presence of ZnCl₂. *Chem. - Eur. J.* **2009**, *15*, 457–468. (b) Piller, F. M.; Bresser, T.; Fischer, M. K. R.; Knochel, P. Preparation of Functionalized Cyclic Enol Phosphates by Halogen-Magnesium Exchange and Directed Deprotonation Reactions. *J. Org. Chem.* **2010**, *75*, 4365–4375. (c) Haag, B.; Mosrin, M.; Ila, H.; Malakhov, V.; Knochel, P. Regio- and Chemoselective Metalation of Arenes and Heteroarenes Using Hindered Metal Amide Bases. *Angew. Chem., Int. Ed.* **2011**, *50*, 9794–9824. (d) Knochel, P.; Benischke, A.; Ellwart, M.; Becker, M. Polyfunctional Zinc and Magnesium Organometallics for Organic Synthesis: Some Perspectives. *Synthesis* **2016**, *48*, 1101–1107.

(8) Bonyhady, S. J.; Jones, C.; Nembenna, S.; Stasch, A.; Edwards, A. J.; McIntyre, G. J. β -Diketiminato-Stabilized Magnesium(I) Dimers and Magnesium(II) Hydride Complexes: Synthesis, Characterization, Adduct Formation, and Reactivity Studies. *Chem. - Eur. J.* **2010**, *16*, 938–955.

(9) Magnesium complexes containing β -diketiminato ligands have also been successfully applied in C–H and C–F activations. For the leading examples see: (a) Davin, L.; McLellan, R.; Kennedy, A. R.; Hevia, E. Ligand-Induced Reactivity of β -Diketiminato Magnesium Complexes for Regioselective Functionalization of Fluoroarenes via C–H or C–F Bond Activations. *Chem. Commun.* **2017**, *53*, 11650–11653. (b) Davin, L.; McLellan, R.; Hernan-Gómez, A.; Clegg, W.; Kennedy, A. R.; Mertens, M.; Stepek, I. A.; Hevia, E. Regioselective Magnesiumation of N-Heterocyclic Molecules: Securing Insecure Cyclic Anions by a β -Diketiminato-Magnesium Clamp. *Chem. Commun.* **2017**, *53*, 3653–3656.

(10) For selected examples on magnesium-catalyzed hydroboration of unsaturated bonds, see: (a) Arrowsmith, M.; Hill, M.; Hadlington, T.; Kociok-Köhn, G.; Weetman, C. Magnesium-Catalyzed Hydroboration of Pyridines. *Organometallics* **2011**, *30*, 5556–5559. (b) Arrowsmith, M.; Hadlington, T.; Hill, M. S.; Kociok-Köhn, G. Magnesium-Catalyzed Hydroboration of Aldehydes and Ketones. *Chem. Commun.* **2012**, *48*, 4567–4569. (c) Mukherjee, D.; Ellern, A.; Sadow, A. D. Magnesium-Catalyzed Hydroboration of Esters: Evidence for a New Zwitterionic Mechanism. *Chem. Sci.* **2014**, *5*, 959–964. (d) Lampland, N.; Hovey, M.; Mukherjee, D.; Sadow, A. D. Magnesium-Catalyzed Mild Reduction of Tertiary and Secondary Amides to Amines. *ACS Catal.* **2015**, *5*, 4219–4226. (e) Manna, K.; Ji, P.; Greene, F.; Lin, W. Metal–Organic Framework Nodes Support Single-Site Magnesium–Alkyl Catalysts for Hydroboration and Hydroamination Reactions. *J. Am. Chem. Soc.* **2016**, *138*, 7488–7491. (f) Mukherjee, D.; Shirase, S.; Spaniol, T.; Mashima, K.; Okuda, J. Magnesium Hydridotriphenylborate $[\text{Mg}(\text{thf})_6][\text{HBPh}_3]_2$: a Versatile Hydroboration Catalyst. *Chem. Commun.* **2016**, *52*, 13155–13158. (g) Rauch, M.; Ruccolo, S.; Parkin, G. Synthesis, Structure, and Reactivity of a Terminal Magnesium Hydride Compound with a Carbatrane Motif, $[\text{Tism}^{\text{PriBenz}}]\text{MgH}$: A Multifunctional Catalyst for Hydrosilylation and Hydroboration. *J. Am. Chem. Soc.* **2017**, *139*, 13264–13267. (h) Barman, M.; Baishya, A.; Nembenna, S. Magnesium Amide Catalyzed Selective Hydroboration of Esters. *Dalton Trans.* **2017**, *46*, 4152–4156. (i) Yang, Y.; Anker, M. D.; Fang, J.; Mahon, M. F.; Maron, L.; Weetman, C.; Hill, M. S. Hydrodeoxygenation of Isocyanates: Snapshot of a Magnesium-mediated C=O bond cleavage. *Chem. Sci.* **2017**, *8*, 3529–3537.

(11) For the use of readily available MgBu_2 as catalyst, see: (a) Magre, M.; Maity, B.; Falconnet, A.; Cavallo, L.; Rueping, M. Magnesium-Catalyzed Hydroboration of Terminal and Internal Alkynes. *Angew. Chem., Int. Ed.* **2019**, *58*, 7025–7029. (b) Jang, Y. K.; Magre, M.; Rueping, M. Chemoselective Luche-Type Reduction of α,β -Unsaturated Ketones by Magnesium Catalysis. *Org. Lett.* **2019**, *21*, 8349–8352. (c) Szewczyk, M.; Magre, M.; Zubar, V.; Rueping, M. Reduction of Cyclic and Linear Organic Carbonates using a Readily Available Magnesium Catalyst. *ACS Catal.* **2019**, *9*, 11634–11639. (d) Magre, M.; Szewczyk, M.; Rueping, M. Magnesium-catalyzed stereoselective hydrostannylation of internal and terminal alkynes. *Org. Lett.* **2020**, *22*, 1594–1598. (e) Magre, M.; Szewczyk, M.; Rueping, M. *N*-Methylation and Trideuteromethylation of Amines via Magnesium-Catalyzed Reduction of Cyclic and Linear Carbamates. *Org. Lett.* **2020**, *22*, 3209–3214.

(12) See for example: (a) Corey, E. J.; Guzman-Pérez, A.; Noe, M. C. Short Enantioselective Synthesis of (–)-Ovalicin, a Potent Inhibitor of Angiogenesis, Using Substrate-Enhanced Catalytic Asymmetric Dihydroxylation. *J. Am. Chem. Soc.* **1994**, *116*, 12109–12110. (b) Movassaghi, M.; Piizzi, G.; Siegel, D. S.; Piersanti, G. Enantioselective Total Synthesis of (–)-Acylfulvene and (–)-Irofulven. *Angew. Chem., Int. Ed.* **2006**, *45*, 5859–5863.

(13) See for example: (a) Johnson, R. A.; Sharpless, K. B. In *Catalytic Asymmetric Synthesis*; Ojima, I., Ed.; Wiley-VCH: New York, 2000; pp 357–398. (b) Ishimaru, T.; Shibata, N.; Nagai, J.; Nakamura, S.; Toru, T.; Kanemasa, S. Lewis Acid-Catalyzed Enantioselective Hydroxylation Reactions of Oxindoles and β -Keto Esters Using DBFOX Ligand. *J. Am. Chem. Soc.* **2006**, *128*, 16488–16489.

(14) For recent review, see: Liu, Y.-L.; Lin, X.-T. Recent Advances in Catalytic Asymmetric Synthesis of Tertiary Alcohols via Nucleophilic Addition to Ketones. *Adv. Synth. Catal.* **2019**, *361*, 876–918.

(15) (a) Falconnet, A.; Magre, M.; Maity, B.; Cavallo, L.; Rueping, M. Asymmetric Magnesium-Catalyzed Hydroboration by Metal-Ligand Cooperative Catalysis. *Angew. Chem., Int. Ed.* **2019**, *58*, 17567–17571. (b) Chatupheeraphat, A.; Rueping, M.; Magre, M. Chemo- and Regioselective Magnesium-Catalyzed *ortho*-Alkenylation of Anilines. *Org. Lett.* **2019**, *21*, 9153–9157.

(16) Ang, N.; Buettner, C.; Docherty, S.; Bismuto, A.; Carney, J.; Docherty, J.; Cowley, M.; Thomas, S. Borane-Catalyzed Hydroboration of Alkynes and Alkenes. *Synthesis* **2018**, *50*, 803–808.

(17) (a) Query, I. P.; Squier, P. A.; Larson, E. M.; Isley, N. A.; Clark, T. B. Alkoxide-Catalyzed Reduction of Ketones with Pinacolborane. *J. Org. Chem.* **2011**, *76*, 6452–6456. (b) Docherty, J. H.; Peng, J.; Dominey, A. P.; Thomas, S. P. Activation and Discovery of Earth-Abundant Metal Catalysts Using Sodium *tert*-Butoxide. *Nat. Chem.* **2017**, *9*, 595–600.

(18) For a seminal contribution, see: (a) Meinwald, J.; Labana, S. S.; Chadha, S. S. Periacid Reactions III. The Oxidation of Bicyclo[2.2.1]heptadiene. *J. Am. Chem. Soc.* **1963**, *85*, 582–585. For recent examples, see: (b) Vyas, D. J.; Larionov, E.; Besnard, C.; Guénee, L.; Mazet, C. Isomerization of Terminal Epoxides by a [Pd-H] Catalyst: A Combined Experimental and Theoretical Mechanistic Study. *J. Am. Chem. Soc.* **2013**, *135*, 6177–6183. (c) Humbert, N.; Vyas, D. J.; Besnard, C.; Mazet, C. An Air-stable Cationic Iridium Hydride as a Highly Active and General Catalyst for the Isomerization of Terminal Epoxides. *Chem. Commun.* **2014**, *50*, 10592–10595.

(19) (a) Falivene, L.; Credendino, R.; Poater, A.; Petta, A.; Serra, L.; Oliva, R.; Scarano, V.; Cavallo, L. SambVca 2. A Web Tool for Analyzing Catalytic Pockets with Topographic Steric Maps. *Organometallics* **2016**, *35*, 2286–2293. (b) Falivene, L.; Cao, Z.; Petta, A.; Serra, L.; Poater, A.; Oliva, R.; Scarano, V.; Cavallo, L. Towards the online computer-aided design of catalytic pockets. *Nat. Chem.* **2019**, *11*, 872–879.